INDUSTRIAL HIGH-RATE (≥4 NM/S) DEPOSITED SILICON NITRIDE WITH LOW SURFACE RECOMBINATION VELOCITIES UNDER OPTIMUM ANTIREFLECTION COATING CONDITIONS

B. Hoex[1,2], A.J.M. van Erven[2], R.C.M. Bosch[2], M.D. Bijker[2], P.J. van den Oever[1], W.M.M. Kessels[1], M.C.M. van de Sanden[1]

[1]Department of Applied Physics, Eindhoven University of Technology, P.O. Box 513, 5600 MB, Eindhoven, email: b.hoex@tue.nl

[2]OTB Solar B.V., P.O. Box 7108, 5605 JC, Eindhoven, The Netherlands

ABSTRACT: High quality surface passivation has been obtained under optimal antireflection coating behavior for silicon nitride films deposited at very high deposition rates of ≥4 nm/s. By extensive process optimization the mass density of our silicon nitride films was increased and the absorption in the UV part of the solar spectrum was reduced. These optimized silicon nitride films were deposited using a commercial inline industrial reactor employing the expanding thermal plasma (ETP) technique and with a nominal throughput of 960 wafers/hour. The low surface recombination velocities of ~50-70 cm/s were obtained on 8.4 Ω cm *p*-type float zone crystalline silicon wafers for the commercially interesting refractive index range of 1.9-2.4. The level of surface passivation was unaffected by a standard industrial firing. Combining the data on surface passivation with the calculated reflection and absorption losses shows that a good level of surface passivation can be obtained under optimal antireflection coating performance.

Keywords: Silicon-Nitride, surface passivation, Industrial Reactor

1 INTRODUCTION

Silicon nitride is now the standard antireflection coating for crystalline solar cells. This coating not only reduces reflection losses, but also can improve the solar cell performance by providing bulk and surface passivation. The current challenges are to obtain a sufficient level of both surface and bulk passivation under optimal antireflection coating conditions for one single silicon nitride film.

A good level of bulk passivation and reduction of reflection losses is already inherently present in the optimization of multi-crystalline solar cell efficiencies, which are dominating today's solar cell market [1]. However, with the current trend toward thinner crystalline silicon wafers and higher solar cell efficiencies [2], surface passivation will also become very important for multicrystalline solar cells. Surface passivation by silicon nitride is well known [3], but the best levels of surface passivation on industrial reactors are generally achieved for silicon nitride films with a refractive index >2.4 which, consequently, show a high level of absorption in the UV part of the solar spectrum, thereby reducing the amount of light entering the solar cell. Recently, a few groups have reported a good level of surface passivation (~50 cm/s on low resistivity *p*-type wafers) on industrial reactors for silicon nitride films with a commercially interesting refractive index of ~2.1 [4, 5]. Though, these good levels of surface passivation were all obtained for silicon nitride films deposited at rates well below 1 nm/s.

In this contribution we will show that we can achieve a good level of surface passivation under optimal antireflection coating performance for our optimized high mass density silicon nitride films deposited at rates ≥ 4 nm/s.

2 EXPERIMENAL DETAILS

2.1 Deposition system

For this study we have used the expanding thermal plasma (ETP) technique as developed by the Eindhoven University of technology and employed in the "DEPx" inline PECVD system of OTB Solar B.V. [6]. As shown in Fig. 1, silicon solar cell wafers are placed on carriers which are propelled electromagnetically through different reactor zones. The carriers, which can hold 2×2 solar cell wafers of 15.7×15.7 cm^2 each, are first heated to the deposition temperature (~425 °C) by infrared radiation in the pre-heating zone. Thereafter, the solar cell wafers enter the deposition zone with three ETP plasma source operating on pure argon. The process gasses NH_3 and SiH_4 are injected into the plasma jet and are cracked down in growth precursors leading to silicon nitride films with a uniformity of ±2.5% over the total carrier width. The deposition pressure is kept constant at ~20 Pa by a two stage roots blower system. The deposition temperature is kept constant during deposition by infrared radiation until the wafers enter the cooling zone. The throughput of the system is 960 solar cell wafers per hour, corresponding to deposition rates of ≥ 4 nm/s.

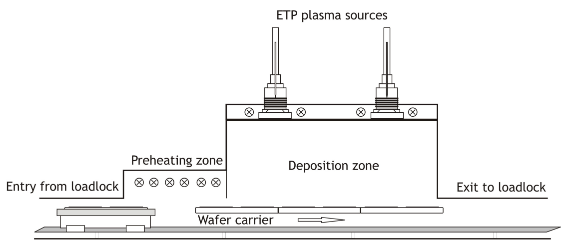

Figure 1: Schematic cross-section of the DEPx silicon nitride deposition system.

2.2 Film analysis

Silicon nitride films of varying refractive index were deposited by changing the NH_3/SiH_4 ratio. The optical properties of the silicon nitride films were analyzed on samples of approximately 80 nm thickness that were deposited on *p*-type c-Si substrates. The samples were analyzed by means of *ex situ* spectroscopic ellipsometry (Woolam M2000) in the 0.7-5 eV energy range. A simple two layer model (bulk film with surface roughness) was used to analyze the data. The dielectric function of the a-SiN:H film was modeled using the Tauc-Lorentz formalism, as proposed by Jellison et al. [7] and the surface roughness was modeled using the Bruggeman effective medium approximation [8].

2.3 Surface passivation

The surface passivation induced by the silicon nitride films was investigated on 8.4 Ω cm *p*-type float zone crystalline silicon wafer with a thickness of 380 μm. The wafers were cleaned using a standard RCA clean with a final HF dip and were coated on both sides with an identical silicon nitride film. The carrier lifetime was determined using a commercial photoconductance tester (Sinton Consulting WCT100 [9]), which was used both in transient as in quasi-steady-state mode. The reflectance of the wafers was taken into account in the measurement.

3 RESULTS AND DISCUSSION

3.1 Process optimization

In previous studies we have identified a relation between the level of bulk passivation and the mass density of the silicon nitride films [10, 11]. Therefore, our process optimization was focused on increasing the mass density of the silicon nitride film.

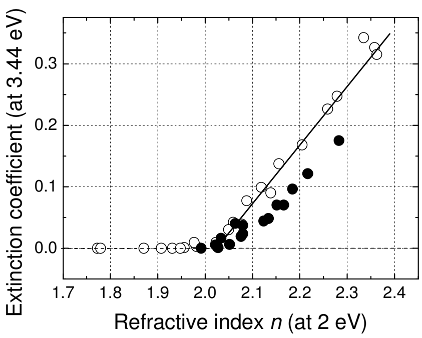

Figure 2: The relation between the refractive index (at a photon energy of 2 eV) and the extinction coefficient (at a photon energy of 3.44 eV) of the silicon nitride films. Films with a high mass density (closed symbols) have a significantly lower extinction coefficient compared to low mass density films (open symbols) for a similar refractive index.

The information on the mass density of the silicon nitride was obtained by means of spectroscopic ellipsometry by considering the relation between the refractive index (at 2 eV) and the extinction coefficient (at 3.44 eV) of the silicon nitride film. These results were corroborated by means of Rutherford backscattering spectroscopy (RBS). From literature it is known that the extinction coefficient is mainly determined by the number of Si-Si bonds in the silicon nitride film. The refractive index of the silicon nitride films is determined both by the mass density and the stoichiometry of the silicon nitride films [12, 13]. As shown in Fig. 2, this results in a specific relation between the extinction coefficient and the refractive index for high and low density silicon nitride films. By extensive process optimization we obtained silicon nitride films with a high mass density (~2.5 g/cm^3 as obtained by RBS). The substrate temperature, and to somewhat lesser extent, the plasma power and gas flows were determined to be the most important process parameters determining the silicon nitride mass density.

Figure 3 shows the reduction of the extinction coefficient as a function of the photon energy that is obtained by our extensive process optimization for a silicon nitride film with a refractive index of n=2.15. It can easily be understood that this reduction in the extinction coefficient of the silicon nitride films is directly beneficial for the saturation current of the resulting solar cell, as the amount of solar radiation absorbed in the antireflection coating is significantly reduced. It should be noted that in comparison with the data presented by Doshi et al. [14] or Jellison et al. [8], our optimized high mass density silicon nitride films exhibit a significantly lower extinction coefficient for silicon nitride films with a similar refractive index. Therefore the absorption losses in our silicon nitride antireflection coating will be significantly reduced.

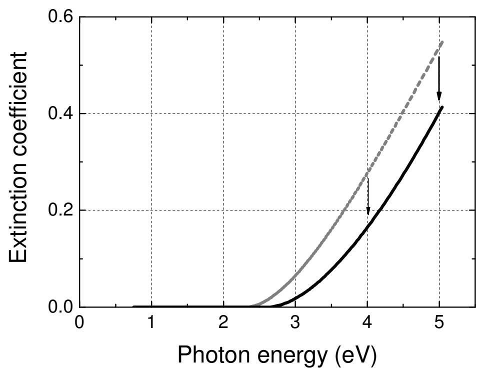

Figure 3: Extinction coefficient as a function of the photon energy as determined by means of spectroscopic ellipsometry for a low mass density silicon nitride film (dashed line) and an optimized high mass density silicon nitride film (solid line) with a refractive index of 2.15.

3.2 Surface passivation by ETP silicon nitride

The surface passivation of the optimized high mass density silicon nitride films was investigated on 8.4 Ω cm *p*-type crystalline silicon wafers. The refractive index of the silicon nitride films was changed by a variation in the silane flow. Effective lifetimes of over 350 μs were measured after coating the wafers with the silicon nitride films (see also [15]). The surface recombination velocity S_{eff} was calculated for an injection level of 2-5×10^{14} cm^{-3} by assuming a realistic bulk lifetime of 4 ms [16]. The upper and lower level of S_{eff} were calculated by assuming an infinite bulk lifetime and the lower limit lifetime limit of 2 ms, respectively. The data presented in Table 1 show that the level of surface passivation is almost constant for the commercially interesting refractive index range of n=1.9-2.4. The surface recombination velocity at the widely used refractive index of n=2.1 is comparable to state-of-the art levels of surface passivation obtained on other industrial reactors, although generally lower resistivity wafers are used. It should be noted that all silicon nitride films were deposited at rates ≥4 nm/s, which is significantly higher compared to other industrial techniques [4, 5, 17].

Table 1: Surface recombination velocity and calculated optimal single layer antireflection coating thickness, reflection loss and absorption loss of the silicon nitride films investigated in this study. The surface passivation was determined on 8.4 Ω cm *p*-type wafers (injection level 2-5×10^{14} cm^{-3}) and the optimal single layer antireflection coating behavior under glass was calculated by using the data obtained by means of spectroscopic ellipsometry and employing the method described by Doshi et al. [14].

n at 2 eV	SRV ±5 (cm/s)	Optimized Thickness (nm)	$<R_w>$ (%)	$<A_w>$ (%)
2.63	413	57.3	4.4	5.9
2.57	249	60.0	4.0	3.8
2.40	71	64.0	3.5	3.4
2.21	48	69.7	3.9	1.4
2.08	65	74.7	4.8	0.1
1.96	50	79.2	5.9	0

In Table 1 also the optimal silicon nitride thickness together with the corresponding reflection and absorption losses for a single layer silicon nitride antireflection coating under glass is given. This data was calculated from the films' optical properties [14] by calculating the reflection and absorption losses weighted by the photon count per wavelength of the standard air mass 1.5 solar spectrum in the 400-1100 nm range. In our simulation we have used a step size of 1 nm instead of 20-30 nm, which was used by Doshi et al. [14]. The data in Table 1 show that for the ideal single layer antireflection coating with a refractive index of 2.1, there are still some absorption losses. Therefore a decrease in the extinction coefficient of the silicon nitride film (as shown in Fig. 2) will directly reduced the absorption losses, hence, improve the antireflection coating behavior.

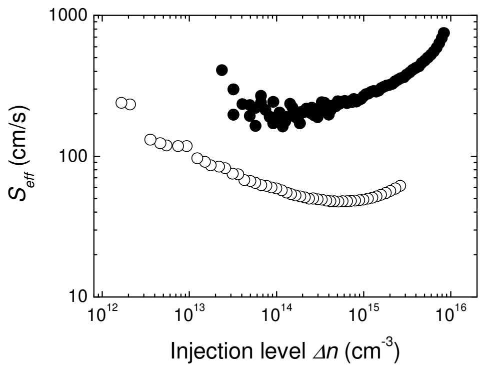

Figure 3: Surface recombination velocity S_{eff} as a function of the injection level for two silicon nitride films with a refractive index of ~2.1 deposited at 350 °C (closed symbols and 425 °C (open symbols), respectively.

Combining the data on the surface passivation and the calculated reflection and absorption losses as presented in Table 1, we can conclude that a good level of surface passivation can be achieved by a single film under optimal antireflection coating performance. These conditions also yield a high level of bulk passivation as recently reported in a separate study [11].

Figure 3 also shows that substrate temperature has a clear impact on the level of surface passivation. The S_{eff} increases to 200 cm/s when the deposition temperature is lowered from ~425 °C to 350 °C. In previous publications also a large impact of the substrate temperature on the level bulk passivation was observed for ETP deposited silicon nitride [18]. The level of surface passivation increases from 50 cm/s to 400 cm/s when the refractive index is increased from 2.4 to 2.6, in contrast to results reported by other authors [19, 20]. This can probably be explained by the fact no process optimization for the deposition of these high index silicon nitride films has taken place.

In a more extensive study we will also show that the surface passivation of our silicon nitride films is not affected by a standard industrial firing step [15].

4 CONCLUSIONS

In this contribution we have shown that the mass density of silicon nitride films can be studied by means of spectroscopic ellipsometry by considering the relation between the refractive index and the extinction coefficient. Eventually, high mass density silicon nitride films (~2.5 g/cm^{-3}) were obtained by extensive process optimization. The surface passivation of these high mass density silicon nitride films was investigated on 8.4 Ω cm *p*-type float zone crystalline silicon wafers. The surface recombination velocity was found to be ~50 cm/s for a broad commercially interesting refractive index range *n* of 1.9-2.4 and was not affected by a standard commercial firing. Combining the data obtained on the surface passivation with the calculated reflection and absorption losses shows that a high level of surface passivation can be obtained under optimal antireflection coating behavior.

ACKNOWLEDGEMENTS

This study has been carried out within the E.E.T. program "HR-CEL" funded by the Netherlands Ministry of Economic Affairs, the Ministry of Education, Culture and Science and the Ministry of Public Housing, Physical Planning and Environment. The research of W.K. has been made possible by a fellowship of the Royal Netherlands Academy of Art and Sciences (KNAW).

REFERENCES

1. G. P. Willeke. *Proceedings of the 19th European Photovoltaic Solar Energy Conference*, Paris, 2004: 383-386.
2. O. Schultz, S. W. Glunz, and G. P. Willeke, *Progress in Photovoltaics: Research and Applications* 2004. **12**(7):553-558.
3. A. G. Aberle, *Progress in Photovoltaics: Research and Applications* 2000. **8**(5):473-487.
4. J. D. Moschner, J. Henze, J. Schmidt, and R. Hezel, *Progress in Photovoltaics: Research and Applications* 2004. **12**(1):21-31.
5. S. Winderbaum, A. Cuevas, F. Chen, J. Tan, K. Hanton, D. Macdonald, and K. Roth. *Proceedings of the*

19th European Photovoltaic Solar Energy Conference, Paris, 2004: 576-579.
6. R. C. M. Bosch, W. T. M. Stals, A. J. M. Van Erven, R. L. J. R. Pennings, and M. D. Bijker. *Proceedings of the 19th European Photovoltaic Solar Energy Conference*, Paris, 2004: 1098-1102.
7. G. E. Jellison and F. A. Modine, *Applied Physics Letters* 1996. **69**(3):371-373.
8. G. E. Jellison, F. A. Modine, P. Doshi, and A. Rohatgi, *Thin Solid Films* 1998. **313**:193-197.
9. R. A. Sinton and A. Cuevas, *Applied Physics Letters* 1996. **69**(17):2510-2512.
10. J. Hong, W. M. M. Kessels, W. J. Soppe, A. W. Weeber, W. M. Arnoldbik, and M. C. M. van de Sanden, *Journal of Vacuum Science & Technology B, Microelectronics and nanometer structures : processing, measurement and phenomena* 2003. **21**(5):2123-2132.
11. A. J. M. Van Erven, R. C. M. Bosch, R. Toelle, O. Voigt, S. Petri, and M. D. Bijker. *Proceedings of the 31st Photovoltaic Specialists Conference and Exhibition*, Lake Buena Vista, 2005
12. J. Robertson, *Philosophical Magazine B-Physics of Condensed Matter Statistical Mechanics Electronic Optical and Magnetic Properties* 1994. **69**(2):307-326.
13. L. Ley, Kärcher, R., Johnson, R.L., *Physical Review Letters* 1984. **53**(7):710-713.
14. P. Doshi, G. E. Jellison, and A. Rohatgi, *Applied Optics* 1997. **36**(30):7826-7837.
15. B. Hoex, A. J. M. Van Erven, R. C. M. Bosch, W. T. M. Stals, M. D. Bijker, P. J. Oever, W. M. M. Kessels, and M. C. M. van de Sanden, *accepted for publication in Progress in Photovoltaics: Research and Applications* 2005.
16. J. Schmidt and A. G. Aberle, *Journal of Applied Physics* 1997. **81**(9):6186-6199.
17. A. W. Weeber, H. C. Rieffe, W. C. Sinke, and W. J. Soppe. *Proceedings of the 19th European Photovoltaic Solar Energy Conference and Exhibition*, Paris, 2004: 1005-1008.
18. J. Hong, W. M. M. Kessels, F. J. H. van Assche, H. C. Rieffe, W. J. Soppe, A. W. Weeber, and M. C. M. van de Sanden, *Progress in Photovoltaics: Research and Applications* 2003. **11**(2):125-130.
19. T. Lauinger, J. Moschner, A. G. Aberle, and R. Hezel, *Journal of Vacuum Science & Technology a-Vacuum Surfaces and Films* 1998. **16**(2):530-543.
20. J. Schmidt, *IEEE Transactions on Electron Devices* 1999. **46**(10):2018-2025.